ANNUAL REVIEWS

Annual Review of Condensed Matter Physics

Superconducting Hydrides Under Pressure

Chris J. Pickard,[1,2] Ion Errea,[3,4,5] and Mikhail I. Eremets[6]

[1]Department of Materials Science & Metallurgy, University of Cambridge, Cambridge CB3 0FS, United Kingdom; email: cjp20@cam.ac.uk

[2]Advanced Institute for Materials Research, Tohoku University, Aoba, Sendai, 980-8577, Japan

[3]Fisika Aplikatua 1 Saila, Gipuzkoako Ingeniaritza Eskola, University of the Basque Country (UPV/EHU), 20018 Donostia/San Sebastián, Spain

[4]Centro de Física de Materiales (CSIC-UPV/EHU), 20018 Donostia/San Sebastián, Spain

[5]Donostia International Physics Center (DIPC), 20018 Donostia/San Sebastián, Spain

[6]Max-Planck Institut für Chemie, Chemistry and Physics at High Pressures Group, 55020 Mainz, Germany

Annu. Rev. Condens. Matter Phys. 2020. 11:57–76

First published as a Review in Advance on September 26, 2019

The *Annual Review of Condensed Matter Physics* is online at conmatphys.annualreviews.org

https://doi.org/10.1146/annurev-conmatphys-031218-013413

Keywords

superconductivity, high pressure, computational materials discovery, structure prediction, electron–phonon coupling

Abstract

The measurement of superconductivity at above 200 K in compressed samples of hydrogen sulfide and in lanthanum hydride at 250 K is reinvigorating the search for conventional high temperature superconductors. At the same time, it exposes a fascinating interplay between theory, computation, and experiment. Conventional superconductivity is well understood, and theoretical tools are available for accurate predictions of the superconducting critical temperature. These predictions depend on knowing the microscopic structure of the material under consideration, which can now be provided by computational first-principles structure predictions. The experiments at the megabar pressures required are extremely challenging, but, for some groups at least, permit the experimental exploration of materials space. We discuss the prospects for the search for new superconductors, ideally at lower pressures.

1. INTRODUCTION

Kamerlingh Onnes's discovery in 1911 that mercury (Hg) abruptly begins to carry a current with no resistance at all when cooled below 4.2 K (1) was a puzzle for decades. Initially referred to as supraconductivity, the temperature at which the resistance suddenly drops is now known as the superconducting critical temperature, T_c. The new superconductors were found to completely exclude external magnetic fields by Meissner & Ochsenfeld in 1933 (2). This is the Meissner effect and, with no classical explanation, it is an essential hallmark of superconductivity. In addition to high temperatures, high magnetic fields destroy the superconducting state. Superconductor applications include the generation of the intense magnetic fields required for magnetic resonance imaging and particle accelerators, as well as superconducting quantum interference devices (SQUIDs), which are capable of measuring minute variations in magnetic fields. The applications are limited, however, by the extremely low temperatures that are needed to access the superconducting state. The quest for high- or even room-temperature superconductors has attained an iconic scientific status. In this review, we describe the discovery of a new family of record-breaking high-temperature superconductors—the high-pressure hydrides. Although the data speak for themselves (see **Figures 1** and **2**), as with all work at the forefront of science, there are a number of outstanding issues and mysteries. We hope that by exploring those in this article, we both put the ongoing research in context for a general reader and inform future research directions. As we discuss below, there is no reason we are aware of that would prevent further increases in T_c to above room temperature.

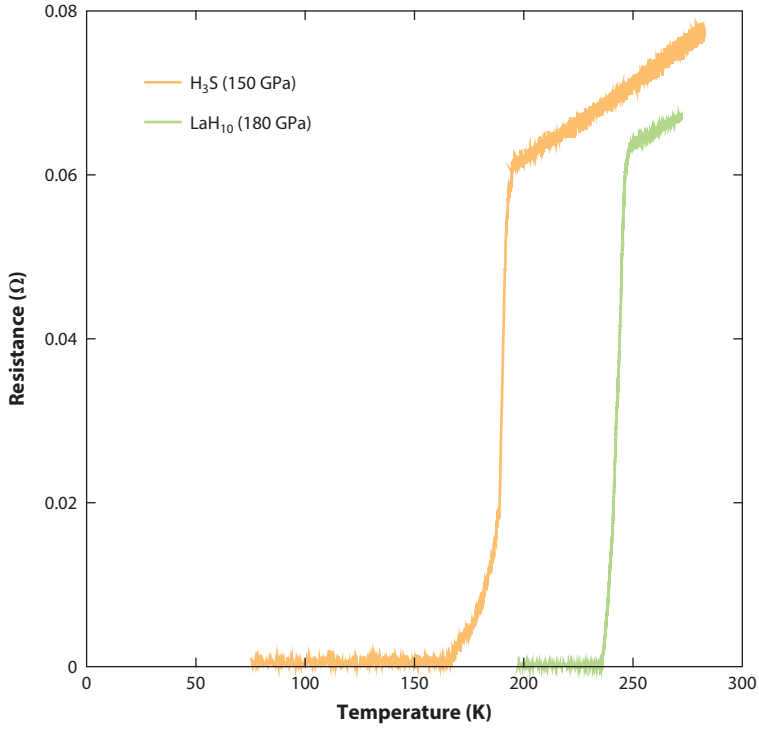

Figure 1

The disappearance of resistance in sulfur and lanthanum high-pressure hydrides at record temperatures. Data taken from References 3 and 4.

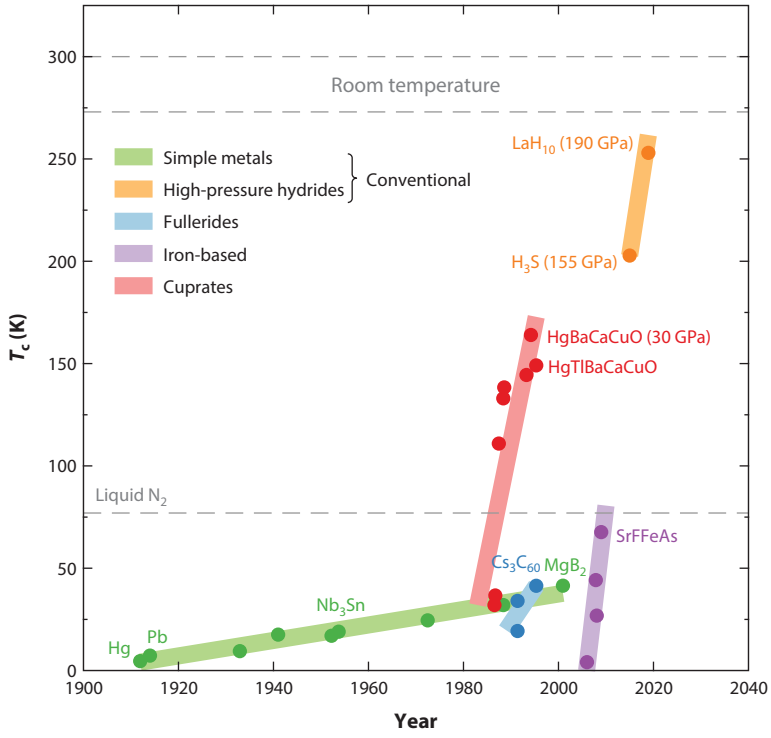

Figure 2

Temporal evolution of the superconducting critical temperature, T_c. Five families of superconductors are highlighted: the simple metals, fullerides, cuprates, iron-based, and high-pressure hydrides. The high-pressure hydrides are conventional superconductors as are the simple metals, whereas the cuprates and iron-based superconductors are unconventional. The pressure at which the measurement has been performed is given in parentheses (if no value is provided, then the value corresponds to ambient pressure). Room and liquid nitrogen temperatures are indicated for reference.

2. A DEVELOPING UNDERSTANDING

From its discovery, superconductivity challenged the existing understanding of the behavior of matter. It had not been (and could not have been using the theoretical tools then available) predicted beforehand. Soon lead (Pb) was found to superconduct at 7.2 K (1), and over the decades that followed many further superconducting materials were identified, culminating in the discovery in 1954 that Nb_3Sn superconducts with a T_c of 18 K (5). Importantly for the many applications that were to follow, Nb_3Sn could tolerate much higher external magnetic fields.

The development of quantum mechanics in the 1920s supplied the missing theoretical tools, and a phenomenological theory of superconductivity emerged, most notably through the work of the London brothers (6). But it would take some time, until the 1950s, before a microscopic picture of superconductivity could be pieced together. In 1950, superconductivity was discovered to depend on the precise masses of the atoms involved (7, 8). This isotope effect suggested to theorists that lattice vibrations, or phonons, play a central role in superconductivity. In 1957, Bardeen, Cooper, and Schrieffer presented their microscopic theory of superconductivity (9, 10). In what would become known as BCS theory, the superconducting state is described in terms of Cooper pairs of electrons, bound through the interaction between the electrons and phonons, which as

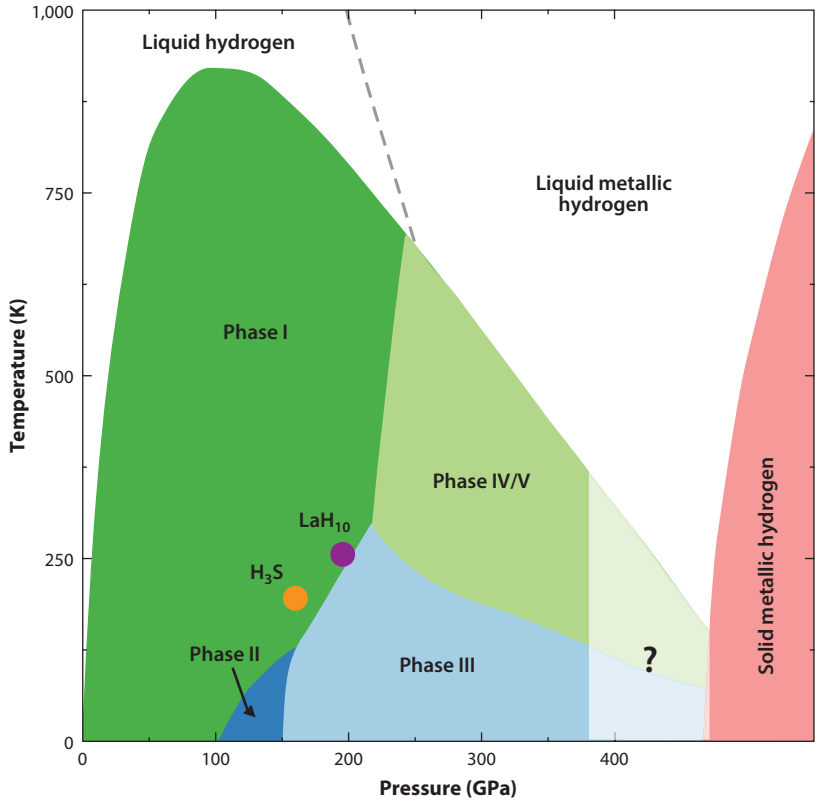

Figure 3

Phase diagram of hydrogen. The superconducting transition temperatures and pressures for the experimentally observed superconducting hydrides, H_3S and LaH_{10}, are marked for reference. Microscopic models for the molecular phases have been provided by first-principles structures predictions (12, 21), but the transition to solid metallic hydrogen is under intense experimental and theoretical scrutiny (shown by the question mark).

bosons condense into a macroscopic quantum state. This theory provides the basis of our understanding of what is now known as conventional superconductivity.

3. SUPERCONDUCTING METALLIC HYDROGEN

It has long been suspected that under sufficient compression hydrogen will join the Group I elements as a metal (11), and **Figure 3** summarizes our current understanding of the phase diagram of hydrogen (12). At low pressures, in phases I, II, and III, molecular hydrogen dominates. At high temperatures and pressures, experiments find a metallic liquid phase (relevant to the gas giant planets in our Solar System and beyond) (13–15). However, at low temperatures there remains considerable controversy, even if recent optical measurements suggest a transition to solid metallic hydrogen at around 495 GPa (16). All theoretical results point to the existence of a solid metallic hydrogen phase at sufficient pressure (12). This might be reached in a semimetallic molecular phase (17, 18) or in an atomic phase (19). Both experiments and theoretical computations are extremely challenging in this transition regime.

Following the introduction of the BCS theory of conventional superconductivity, Ashcroft proposed in 1968 that solid metallic hydrogen, if it could be made, would be a high-temperature superconductor (20). The BCS expression for the superconducting T_c is

$$T_c = 0.85\Theta_D e^{-1/N(0)V}, \quad 1.$$

where Θ_D is the Debye temperature (derived from the highest-frequency vibrational mode in the system), $N(0)$ is the electron density of states (eDOS) at the Fermi level, and V is an effective electron–phonon attractive interaction. The low mass of the proton ensures that metallic hydrogen has a high Debye temperature, and assuming a reasonable value for $N(0)V$, Ashcroft predicted the T_c to be very high.

Though at that time metallic hydrogen was not within reach, Ashcroft's ideas were immediately put to work in the hunt for superconducting metallic hydrides at ambient pressures. However, the compounds investigated were either not superconducting, like the lanthanum hydrides (22, 23), or only superconducting with T_c around 10 K (24–26). Little further progress was made, and attention was soon to be directed to a new class of superconductors.

4. HIGH-TEMPERATURE SUPERCONDUCTIVITY

In 1986, research into superconductivity underwent a revolution due to the discovery of very high-transition temperatures in a new class of materials: the cuprates. Over a relatively short period of time the transition temperatures rocketed from around 30 K in $Ba_xLa_{5-x}Cu_5O_{5(3-y)}$, the result announced by Bednorz & Müller (27), to 164 K in HgBaCaCuO (28) at 30 GPa (see **Figure 2**). There was great optimism that room-temperature superconductors were within our grasp. However, it soon became clear that these high-temperature superconductors did not follow the same rules as the conventional BCS superconductors. These unconventional superconductors demanded a new theoretical framework, one about which, despite intense effort and the deployment of many creative ideas (29), there is still no general consensus. The cuprates have more recently been joined by the iron-based superconductors (30, 31), but in the face of the diminishing increases in T_c through doping or pressure, and despite providing a guide to the rich landscape of emergent phases in quantum matter (32), theory has not been in the position to provide a road map to room-temperature superconductivity based on these unconventional superconductors.

5. NEW HOPE FOR THE CONVENTIONAL SUPERCONDUCTORS

The discovery of the surprisingly high T_c, 39 K, of MgB_2 in 2001 (33) reminded the community of the potential of the conventional superconductors. The low cost of MgB_2 has made it an important superconductor for applications (34). However, it appears to have been an isolated success, and subsequently discovered conventional superconductors (such as CaC_6; 35) have not surpassed it.

In 2004, Ashcroft returned to his earlier ideas, this time explicitly suggesting that compounds with a high hydrogen content might be, in effect, chemically precompressed metallic hydrogen (36). With Hoffmann in 2006, a concrete proposal was made (37), and the era of a theory-and-computation-led hunt for high-temperature superconductors was upon us. The three developments that were central to this were (*a*) the reliable prediction of the stable structures of the hydrides under pressure, (*b*) the accurate computation of their superconducting properties, and (*c*) their experimental realization in diamond anvil cells (DACs) (see **Figure 4**). We focus on the interplay between experiment, theory, and computation that has led to the new class of superconducting materials: the dense hydrides.

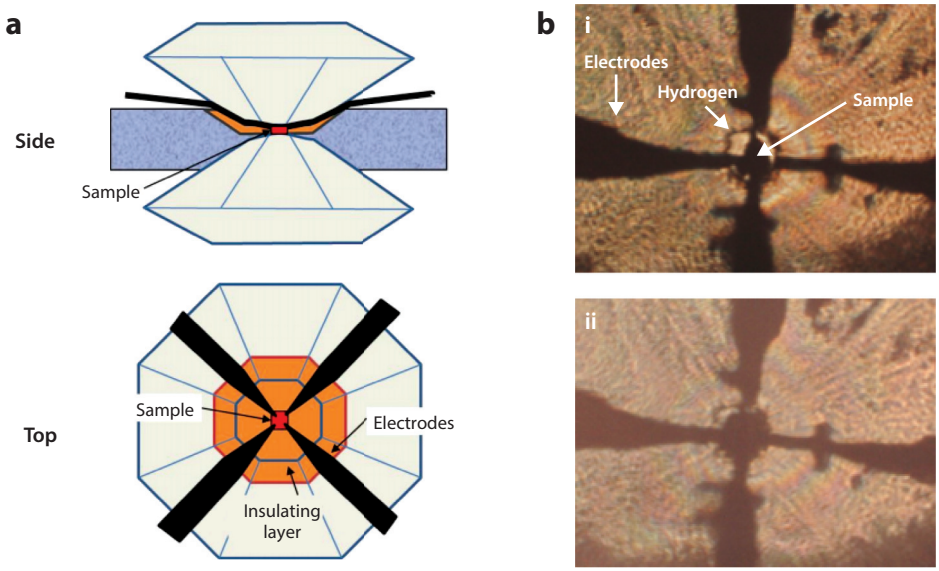

Figure 4

Experimental synthesis and characterization of dense hydrides in (*a*) a diamond anvil cell (DAC). (*b*) Photographs of the lanthanum hydride sample at 143 GPa (pressure determined from the shift of the Raman active vibron peak of hydrogen surrounding the sample). (*i*) Before laser heating and (*ii*) after laser heating the sample, strongly expanded due to absorption of hydrogen. Panel *a* adapted from Reference 38.

6. DENSITY FUNCTIONAL THEORY

In principle, solving the equations governing quantum physics—Schrödinger's or Dirac's equations—would allow us to anticipate the nature and properties of any material under conditions of our choice. In practice this is too difficult, or computationally expensive. It is typically assumed that the atomic nuclei are so much more massive than the electrons that the Born–Oppenheimer approximation holds, meaning only the lighter electrons need be treated quantum mechanically. This simplifies computation considerably, but for the hydrides (because of the low mass of hydrogen) this approximation can break down.

With Hohenberg, Kohn showed that the electronic charge density was sufficient to determine the ground-state energy of a system (39). This energy can be written as a functional (or function of a function) of the density, hence density functional theory (DFT). This put the earlier ideas of Thomas and Fermi on a solid theoretical footing, but the exact form of the appropriate functional remained, and remains, unknown. To create a useful computational scheme, Kohn & Sham rewrote the charge density in terms of a set of functions reminiscent of independent particle orbitals (40). This meant that a large portion of the kinetic energy could be calculated precisely, and the remainder was combined with the other unknown parts of the functional, the exchange and correlation term. The Kohn–Sham equations include the following:

$$(T + V_{\mathrm{KS}})\,|\phi_i\rangle = \varepsilon_i |\phi_i\rangle. \qquad 2.$$

Here, T is the electron kinetic energy operator, V_{KS} the Kohn–Sham potential, and ε_i and $|\phi_i\rangle$ are the energy and wave function of the i-th Kohn–Sham orbital, respectively. A drawback is that the exchange–correlation part of V_{KS} is unknown and needs to be approximated. The wide adoption

of DFT that we see today has depended on the development of reliable approximations to the exchange and correlation term (41).

7. STRUCTURES FROM FIRST PRINCIPLES

The computational discovery of materials with previously unknown structures became practical with the introduction in 2006 of methods for general first-principles structure prediction (42). These evolutionary (43) and random structure searching (44) approaches employed pragmatic strategies for exploring low-lying configurations of the DFT energy landscapes generated by state-of-the-art plane wave and pseudopotential codes (45, 46).

The repeated stochastic generation of structures, followed by careful DFT-based relaxations to the nearby local minima of the Born–Oppenheimer potential, is the starting point for successful first-principles approaches to structure prediction. If no other steps are taken, this is known as *ab initio* random structure searching, and it benefits from parallelism and broad exploratory searches. A particular emphasis is placed on the generation of sensible initial structures, in which chemical ideas such as coordination, distances, units, and symmetry are imposed (47). Evolutionary (43) and swarm approaches (48) build subsequent moves on what has already been learned about the energy landscape, trading some simplicity, parallelism, and exploratory power for a greater exploitation of this hard-won information. The different approaches appear to be complementary, and the combined application of random and swarm-based searches has been particularly powerful in the study of the hydrides (49, 50). In combination with general purpose plane wave DFT codes (45, 46, 51), databases of reliable potentials covering the entire periodic table (52), and the arrival of commodity multicore CPUs, first-principles structure prediction has now become widespread and almost routine (53).

The same trends in software and computer architecture have led to high-throughput approaches to materials informatics (54). These, at least initially, depend on the availability of curated databases of crystal structures. However, they have not yet proven useful to the study of the dense hydrides, whose crystal structures are typically not found in existing databases. Indeed, even for those structure prototypes that might be available in a database, using modern structure prediction methods, it can be easier, faster, and more reliable to rediscover the structures, rather than draw candidates from a database, relax and compute their ground-state energies from first principles, and sort among them.

There have been many striking applications of first-principles structure prediction, in particular to high-pressure phase transitions (55). In the absence of experimentally derived information, structure prediction has provided the most reliable microscopic models of dense hydrogen itself. Using random search, a convincing model of phase III was introduced (21), which exhibited the observed strong infrared activity. Mixed phases were also encountered in the search, and these anticipated the experimental discovery of phase IV (56, 57). As an end-member, good models for the high-pressure phases of hydrogen have proved important in the search for the binary dense hydrides. Using Maxwell constructions, or convex hull plots (see **Figure 5**), the stability of these binary (or ternary and above) hydrides can be straightforwardly assessed (58).

8. SUPERCONDUCTORS FROM FIRST PRINCIPLES

In the known superconducting hydrides, the coupling mechanism driving the condensation of the Cooper pairs is the well-known electron–phonon interaction: They are conventional superconductors. This means that it is possible to perform first-principles calculations of their superconducting critical temperatures using established theoretical and computational approaches.

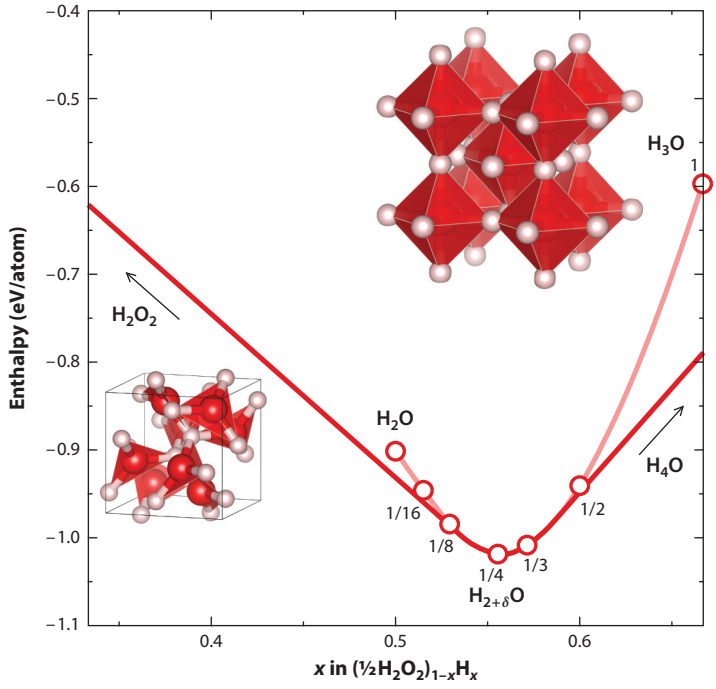

Figure 5

Convex hull for the hydrogen–oxygen system at 6 TPa. Under these extreme pressures, water (H_2O) decomposes into hydrogen peroxide (H_2O_2) and a hydrogen-rich phase ($H_{2+\delta}O$). At $\delta = 1$ the H_3O structure is the same as the superconducting $Im\bar{3}m$ H_3S phase. The stable compositions lie on the convex hull, and H_3O is seen to be unstable to a density-of-states-lowering change in composition (59).

Exploiting the dramatic increase in available computational power, these first-principles calculations have been central to the characterization and understanding of the properties of superconducting hydrides and, importantly, to the prediction of new high-T_c compounds.

Once the crystal structure for a given material is known, three basic ingredients are required to calculate its T_c within DFT: the Kohn–Sham energies ε_i and wave functions $|\phi_i\rangle$, where i labels a given electronic state; the phonon frequencies ω_μ, with a mode index μ; and the electron–phonon matrix elements (60),

$$g_{ij}^{\mu} = \langle \phi_i | \frac{\partial V_{\mathrm{KS}}}{\partial u^{\mu}} | \phi_j \rangle. \qquad 3.$$

In the above, u^μ is the atomic displacement according to the normal mode μ. Phonon frequencies are now routinely calculated within the harmonic approximation, truncating the Born–Oppenheimer energy surface at second order. The harmonic force constants are calculated by making use of linear response theory (61) or finite difference approaches (62). The electron–phonon matrix elements are obtained analogously from linear response (61, 63) or finite difference methods (62, 64).

Bringing together the Kohn–Sham energies, phonon frequencies, and electron–phonon matrix elements, the Eliashberg function $\alpha^2F(\omega)$ can be directly evaluated as a phonon density of states weighted by the electron–phonon interaction at the Fermi energy ε_F:

$$\alpha^2 F(\omega) = \sum_{ij\mu} |g_{ij}^{\mu}|^2 \delta(\omega - \omega_\mu) \delta(\varepsilon_i - \varepsilon_F) \delta(\varepsilon_j - \varepsilon_F). \qquad 4.$$

This function is central to the prediction of T_c in superconductors. The electron–phonon coupling constant is calculated as

$$\lambda = 2\int_0^\infty d\omega \frac{\alpha^2 F(\omega)}{\omega}, \quad 5.$$

and it measures the strength of the attractive interaction between the electrons and the phonons. The semiempirical McMillan equation (65),

$$k_B T_c = \frac{\hbar\omega_{\log}}{1.2}\exp\left[-\frac{1.04(1+\lambda)}{\lambda-\mu^*(1+0.62\lambda)}\right], \quad 6.$$

is typically used to predict the critical temperature. The average logarithmic frequency $\omega_{\log}$ can be computed from

$$\omega_{\log} = \exp\left[\frac{2}{\lambda}\int_0^\infty d\omega \frac{\alpha^2 F(\omega)}{\omega}\ln\omega\right], \quad 7.$$

and μ^* is the so-called Coulomb pseudopotential, which accounts for the repulsive electron–electron interaction. The latter is usually taken as a parameter around 0.1, though it can also be explicitly calculated (66).

This approach has been successful in accurately computing the T_c of several compounds (67–69), but it suffers from limitations that are particularly important for the superconducting hydrides. First, the McMillan equation tends to systematically underestimate T_c for strongly coupled superconductors ($\lambda > 1$) (65). These difficulties can be overcome by directly solving the many-body Migdal–Eliashberg equations for the superconducting gap (70) or by adopting a DFT for superconductors (71), which is an extension of DFT accounting for the superconducting state. As an example, the T_c predicted with the McMillan equation for H_3S in the cubic $Im\bar{3}m$ phase at 200 GPa is 125 K, whereas the Migdal–Eliashberg equations yield 194 K ($\lambda = 1.84$ in this case) (72).

A second important limitation is the breakdown of the harmonic approximation used to calculate the phonon frequencies. The electron–phonon coupling constant strongly depends on the phonon frequencies: $\lambda \sim \sum_\mu 1/\omega_\mu^2$. If anharmonic effects significantly renormalize the phonon frequencies, λ can be substantially modified, and, as a result, so can T_c. Because of the low mass of hydrogen and its large quantum fluctuations from equilibrium, substantial anharmonic corrections to T_c have been predicted in many superconducting hydrides and some candidate phases of hydrogen (72–78), though not for all (79). In **Figure 6**, we illustrate the effect of anharmonicity with the calculation performed in Reference 75 for PtH at 100 GPa in the hexagonal close-packed structure that has been synthesized experimentally at lower pressures (80). There is strong anharmonic hardening of the phonon energies in this compound, which is mostly associated with the hydrogen-related modes, and a consequent suppression of λ and T_c, by greater than an order of magnitude for the superconducting critical temperature.

9. THE ROUTE TO SUPERCONDUCTING HYDRIDES

Ashcroft and Hoffmann's first suggestion that compressed silane (SiH_4) might take us to metallic superconducting hydrogen (37), at lower pressures than pure H_2, was backed up by first-principles computations of its expected properties (37). The structures investigated were derived largely from chemical intuition, and using the newly developed first-principles structure prediction techniques it was quickly shown that there were more stable phases that were expected to be semiconducting and, hence, poor candidates for superconductivity (44). Experiments confirmed these structural predictions, and the T_c was found to be low (81). Methane (CH_4) and germane (GeH_4) were

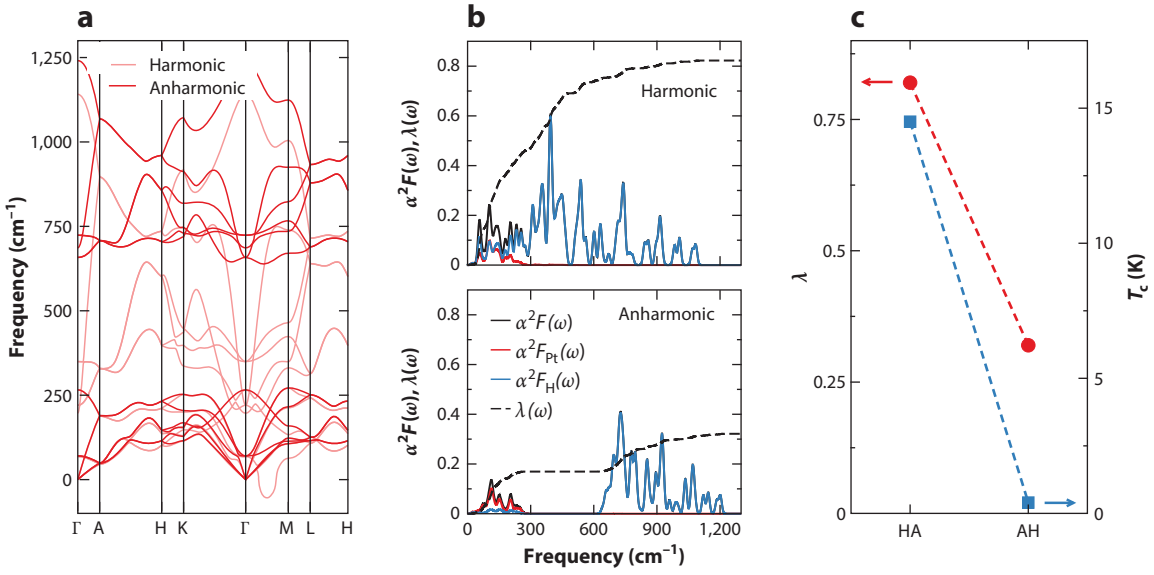

Figure 6

(*a*) Phonon spectra of PtH in the hexagonal close-packed structure at 100 GPa for the harmonic and anharmonic cases. (*b*) Eliashberg function $\alpha^2F(\omega)$ and the integrated electron–phonon coupling $\lambda(\omega) = 2\int_0^\omega d\Omega\alpha^2F(\Omega)/\Omega$ in the harmonic and anharmonic cases. The decomposition of $\alpha^2F(\omega)$ into H and Pt contributions is included. (*c*) The calculated λ and T_c in the harmonic and anharmonic calculations. Abbreviations: AH, anharmonic; HA, harmonic. Data from Reference 75.

suggested (82), but they also did not exhibit high-temperature superconductivity. The hydrogen storage materials [$LiBH_4$, $NaBH_4$, NH_3BH_3, $Si(CH_3)_4$] were obvious candidates, given their high hydrogen content, but they resisted metallization to high pressures. One of them, aluminum hydride (AlH_3) was found to metallize, both theoretically (83) and experimentally (84), but did not superconduct at 20 K as predicted by the calculations. This was later explained to be a result of strong anharmonic effects (73). Despite these disappointments, some groups persisted and went on to make remarkable predictions, most notably that CaH_6 would have a T_c of 235 K at 150 GPa (85). The structures of some of these compounds are shown in **Figure 7** and their eDOS in **Figure 8**.

10. DISCOVERY OF SUPERCONDUCTIVITY IN HYDROGEN SULFIDE

In the face of the early failures, the experimental quest continued. H_2S was selected as it is widely available and had been predicted to superconduct with a T_c around 80 K at high pressure (86) by a group with a good track record, having successfully anticipated the emergence of transparent sodium under compression (87). It was a good choice, as superconductivity with T_c 50–60 K was found, in reasonable agreement with theory. With that measurement already a record for conventional superconductors, further inspection revealed a strong increase in T_c with pressure, up to about 150 K. Serendipitously, it was noticed that not only pressure but also increasing temperature led T_c to soar, suggesting that a kinetic transformation was at play. The sample was then deliberately heated, and T_c further increased, stabilizing at around 200 K. It was suspected that H_2S disproportionated with temperature, likely transforming to H_3S plus sulfur. A similar decomposition had been predicted in water (H_2O) at terapascal pressures (see **Figure 5**), a chemical analog for H_2S.

This observed superconductivity was characterized by zero resistance, a shift of T_c to lower temperatures with applied magnetic field, and a strong isotope effect (through the replacement of

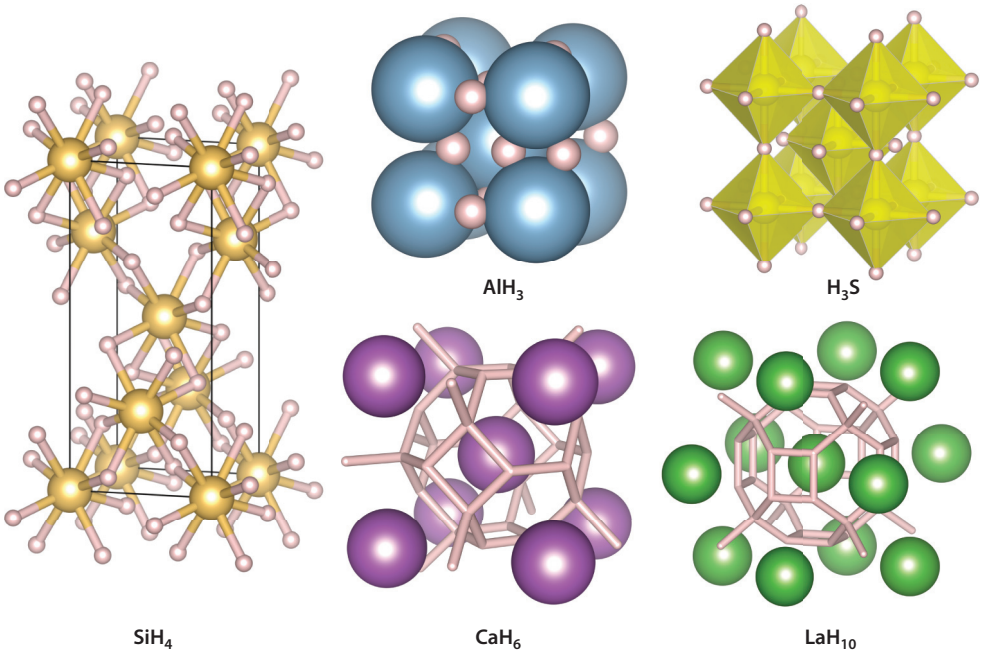

Figure 7

Gallery of key hydride structures. SiH_4 and AlH_3 at 100 GPa, and H_3S, CaH_6, and LaH_{10} at 200 GPa. The H_3S structure consists of interpenetrating ReO_3 lattices. CaH_6 and LaH_{10} exhibit a striking hydrogen framework structure and have been referred to as clathrates or sodalite-like.

H_2S with D_2S) that pointed to conventional superconductivity. Crucially, the Meissner effect was observed. This required the development of a new high-pressure technique: the use of a sensitive SQUID magnetometer. In order to accommodate a SQUID, DACs smaller than 9 mm in diameter were required. Such tiny DACs had previously worked up to 15 GPa, and fortunately they also did so at 200 GPa, providing the final convincing evidence of superconductivity (3). The fact that independent calculations suggested, almost at the same time, that H_3S may be a high-T_c compound (88) provided further support. The predictions and experiments were consistent.

11. A THEORETICAL UNDERSTANDING EMERGES

This experimental discovery of superconductivity at 203 K in hydrogen sulfide (3) stimulated further intense theoretical work, which has proven crucial to the full characterization and understanding of its properties. Variable stoichiometry crystal structure predictions clearly determined that H_2S is not thermodynamically stable above 50 GPa and that it decomposes mainly into H_3S and S, as suggested by the experiments, although other decomposition mechanisms have also been considered (49, 72, 90). Among all the possible compounds resulting from the decomposition, first-principles calculations soon determined that only H_3S could provide such an extraordinary T_c (49, 72, 76, 77, 91, 92). All other possibilities yielded values of λ that were too low. This picture that H_2S decomposes yielding H_3S is further supported by the fact that the rise in T_c with increasing pressure observed (3) is consistent with the theoretical T_c provided by a gradual transformation of H_2S into H_3S (93).

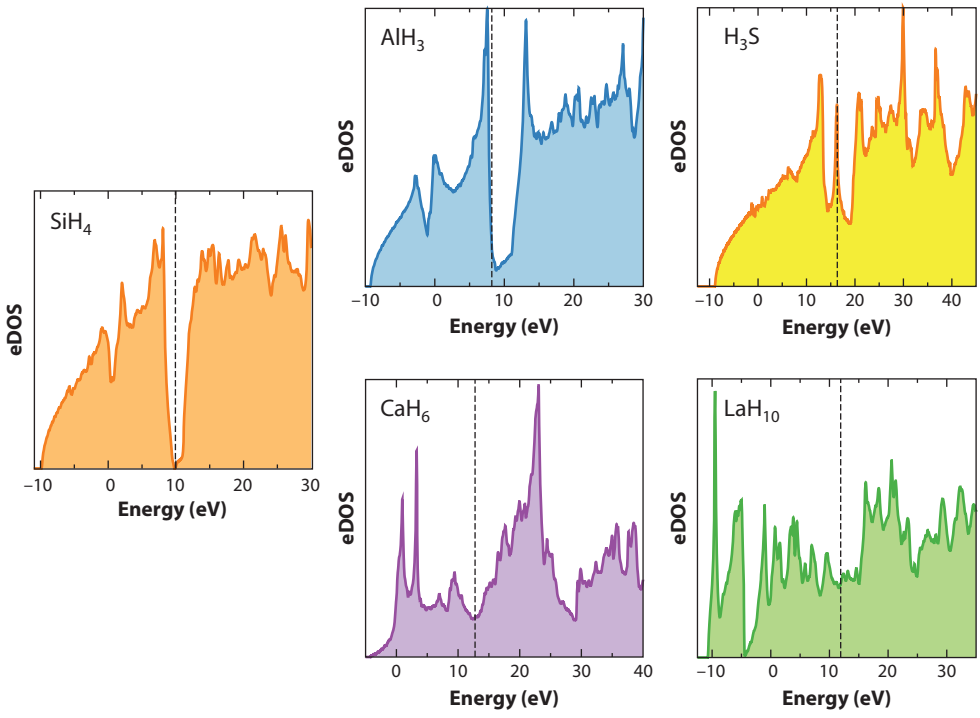

Figure 8

The eDOS for SiH_4 (44) at 100 GPa, AlH_3 (83, 84) at 100 GPa, H_3S (88) at 200 GPa, CaH_6 (85) at 200 GPa, and LaH_{10} (50, 89) at 200 GPa. The Fermi level, ε_F, is indicated by a vertical dashed line. Note that a small gap opens up for SiH_4, and so it is not expected to superconduct (44). AlH_3 is metallic (83, 84), but anharmonicity destroys high T_c (73). H_3S exhibits a peak in the eDOS close to ε_F, pointing to its remarkable properties. Both CaH_6 and LaH_{10} are good metallic hydrides. Abbreviation: eDOS, electron density of states.

The phase sequence predicted for H_3S suggests a *Cccm* (88) or *C*2/*c* (49) structure below 112 GPa, both formed of H_2S and H_2 units that cannot explain the large T_c, a rhombohedral *R*3*m* phase between 112 GPa and approximately 175 GPa, and a cubic $Im\bar{3}m$ phase above (49, 88). As shown in **Figure 9**, the H atoms in the $Im\bar{3}m$ phase sit exactly halfway between two sulfur atoms forming a structure with full cubic symmetry. At lower pressures, the hydrogen atoms move to an off-center position, forming a short H−S covalent bond and a longer H···S hydrogen bond, lowering the symmetry to *R*3*m*. The displacive transition from $Im\bar{3}m$ to *R*3*m* is driven by the softening of a phonon mode at the Γ point.

The above sequence of phases was determined by neglecting the contribution of the ionic fluctuations to the energy, the quantum zero-point energy, and so a classical prediction. As discussed in Section 8, quantum fluctuations mean that hydrogen atoms vibrate with a large amplitude from equilibrium even at absolute zero, which can lead to a substantial anharmonic renormalization of the phonon frequencies. As shown in Reference 76, once the zero-point energy is included in the calculations, the *R*3*m* is no longer the ground-state structure below 175 GPa, and the cubic $Im\bar{3}m$ is favorable even if it is dynamically unstable in the harmonic approximation. Anharmonicity stabilizes the phonons of the cubic phase and yields T_c values in agreement with experiments (see **Figure 9**) (76). The highest temperature at which superconductivity is observed in H_3S occurs in a structure with hydrogen bonds symmetrized by quantum effects. Once these quantum

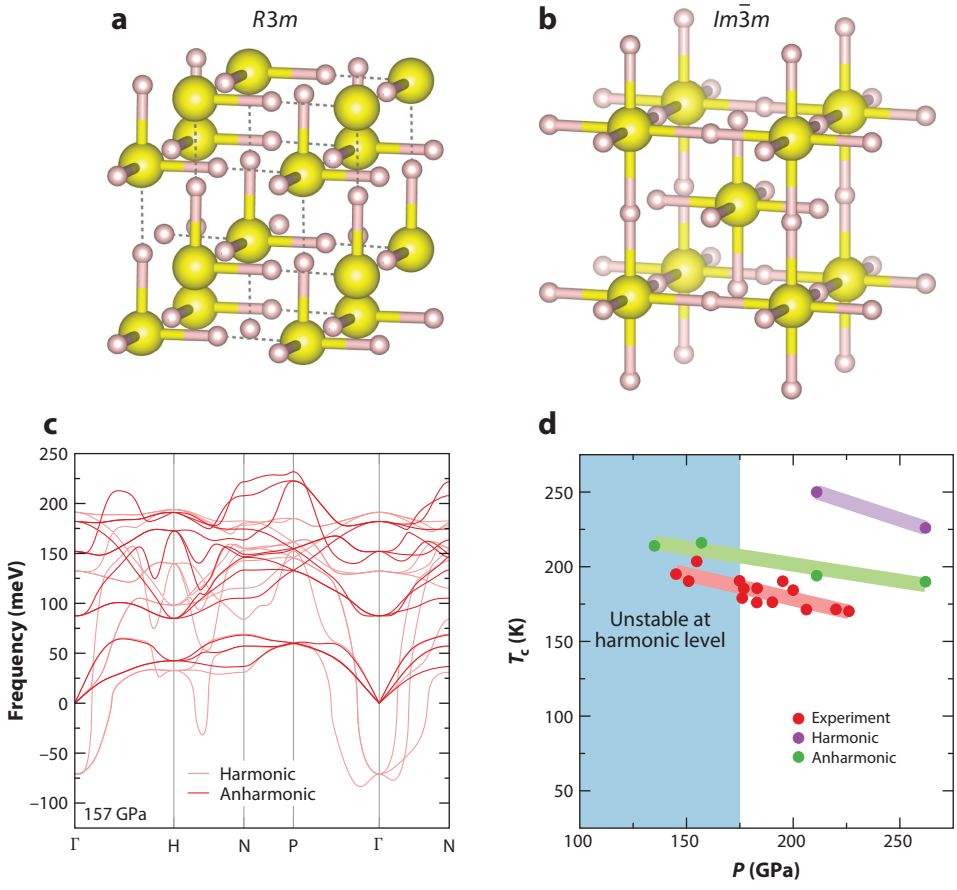

Figure 9

Crystal structure of (*a*) *R*3*m* and (*b*) *Im*$\bar{3}$*m* phases of H_3S. (*c*) Phonon spectra of *Im*$\bar{3}$*m* H_3S at 157 GPa and (*d*) T_c as a function of pressure of *Im*$\bar{3}$*m* H_3S calculated in the harmonic approximation and including anharmonicity. In panel *d*, the blue region describes the pressures at which *Im*$\bar{3}$*m* H_3S is not stable in the harmonic approximation. The experimental data for H_3S in Reference 3 is provided for reference. The theoretical data for this figure is taken from Reference 76.

anharmonic effects are correctly included, the transition between the *Im*$\bar{3}$*m* and *R*3*m* phases is estimated to be between 91 and 114 GPa (94).

12. FURTHER EXPERIMENTAL CHARACTERIZATION

Early X-ray diffraction measurements (95), performed on a compressed H_2S sample, confirmed its decomposition yielding H_3S with a bcc arrangement of the S atoms but could not distinguish between the *R*3*m* and *Im*$\bar{3}$*m* phases. Hydrogen atoms are very weak scatterers and their position cannot easily be determined by XRD. T_c was measured on further pressure release and showed a pronounced kink at 150 GPa, which could signal the occurrence of the *Im*$\bar{3}$*m* → *R*3*m* transition (95). Two more recent experimental studies synthesized clean H_3S by annealing a sulfur sample in a DAC loaded with H_2 gas. Goncharov et al. (96) confirmed the theoretically predicted *Cccm* → *R*3*m* → *Im*$\bar{3}$*m* structural sequence. The cubic *Im*$\bar{3}$*m* was directly synthesized at

high pressure, and subsequent pressure release led to the appearance of a rhombohedral distortion compatible with the $R3m$ phase at 140 GPa, which remained metastable down to 70 GPa, where it transformed upon annealing to the $Cccm$ structure. The observed rhombohedral distortion is much larger than that expected theoretically (94), which could be due to slight nonhydrostatic conditions in the DAC. This raises hopes of preserving the cubic $Im\bar{3}m$ structure and its large T_c to even lower pressures. By annealing H_2 and S at lower pressures instead, Guigue et al. (97) were only able to synthesize $Cccm$ H_3S, which remained metastable up to 160 GPa. Taken together, these results suggest that the transition between the $Cccm$ phase to the $R3m$ or $Im\bar{3}m$ phases is strongly affected by large kinetic barriers. This observation has important implications for the predictability of high-pressure hydrides.

The superconducting state of H_3S has been further characterized by optical and magnetic measurements (38, 98, 99). Capitani et al. (38) found evidence for the presence of a large electron–phonon mediated superconducting gap in reflectivity measurements, which was in agreement with the reflectivity calculated with the anharmonic $\alpha^2F(\omega)$ in Reference 76. Recent magnetic measurements up to 65 T at 155 GPa (99) show a critical magnetic field consistent with a strongly coupled superconductor with $\lambda \sim 2$, a value in agreement with first-principles computations (76).

13. LANTHANUM HYDRIDES AND BEYOND

The discovery of superconductivity above 200 K in H_3S in 2015 showed that hydrides can indeed be high-T_c superconductors. At the same time, it clearly illustrated how fruitful the combination of theory and experiment can be in the characterization and understanding of these materials. Soon, evidence that PH_3 superconducts at 100 K and 200 GPa was reported (105). First-principles calculations, however, show that PH_n compounds are not thermodynamically stable with respect to the decomposition into phosphorus and hydrogen, suggesting that superconductivity might have occurred in a metastable state in a compound with an unknown stoichiometry (106).

More recently, evidence for superconducting transitions as high as above 250 K have been reported in a lanthanum hydride at around 150–200 GPa by two independent groups (4, 101, 107). The synthesis was achieved by directly annealing in the DAC La and H_2 gas (4, 107) or using BH_3NH_3 as the hydrogen source (101). The latter option dramatically simplifies the experiment as only solid samples are used, even if the synthesis is less well controlled. In any case, a severe experimental difficulty encountered is that phases with different structures and stoichiometry are synthesized at nearly the same pressure–temperature conditions, and the final product depends on the kinetics of the transformations. Based on the volume per formula unit, a stoichiometry of around LaH_{10} has been estimated (4, 108). The most probable candidate for such an extraordinary value of T_c is a hydrogen clathrate structure with LaH_{10} stoichiometry and space group $Fm\bar{3}m$ (see **Figure 7**), previously predicted to be a high-T_c superconductor by first-principles calculations (50, 89). For this structure a pure superconducting metallic hydrogen lattice exists, to which the host La atoms donate electrons (89). XRD measurements are consistent with this phase (4, 108). Nevertheless, different values of T_c have been observed (4, 107), and XRD experiments find very different phases for the hydrogen and deuterium compounds (4). Further theoretical calculations that accurately account for quantum anharmonic effects are thus needed to clarify the phase diagram and the superconducting nature of these hydrides.

By now there are a very large number of hydrides that have been predicted theoretically to be thermodynamically stable and exhibit a high T_c. **Figure 10** summarizes many of these predictions, which are discussed in detail in Reference 104. Even if such predictions might once have been unbelievable, ignored, or criticized by part of the superconducting community (109), it is now clear

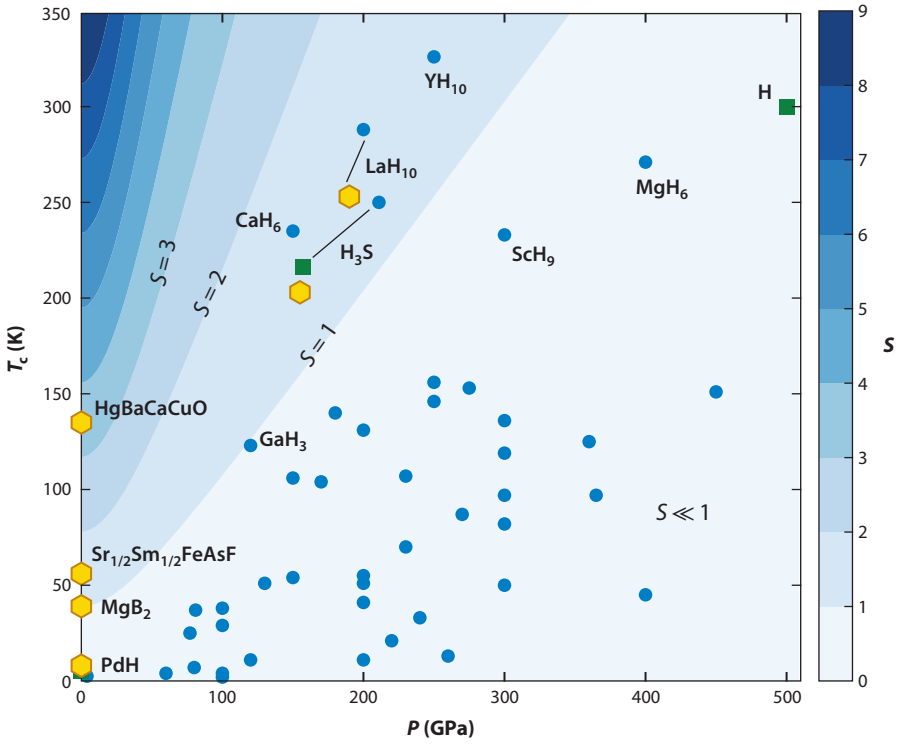

Figure 10

Superconducting critical temperature, T_c, as a function of the pressure at which it has been calculated or measured for different hydrides. Yellow hexagons correspond to experimental measurements (3, 33, 100–103). Green squares correspond to first-principles calculations including anharmonic effects (72, 74, 79). All other small circles correspond to predictions at the harmonic level as summarized in table 1 of Reference 104, except for H_3S (76). The colored contours correspond to the figure of merit S proposed in Equation 8.

that there is plenty of room for further groundbreaking experimental discoveries, although experimental progress is slow as compared to theory and computation. We could ask ourselves, why should this be the case? One obvious reason is the difficulty of the experiments. It could be because the synthesis of these dense hydrides is hindered by large kinetic barriers due to the making and breaking of hydrogen dimers or simply because many of these predictions are inaccurate, in particular, because the quantum nature of the hydrogen atoms is usually neglected, or because of the intrinsic limitations of DFT, or the extensiveness of the structural searches.

14. DISCUSSION

There is continuing interest in the experimental results for the lanthanum hydrides, and we can expect further experimental investigations. At the same time, theoretical groups will attempt to refine our microscopic understanding of this system, in particular exploring the impact of the quantum dynamical behavior of the protons on structure, stability, and superconductivity. And no doubt the computational search for new candidates will continue. It is possible that the true structures of the hydrides are more complex than the fairly small unit cells typically investigated, and our understanding of the binary hydrides may be refined. Beyond that, the ternaries beckon.

Many questions, as well as challenges and opportunities, remain. What do these recent successes in the superconducting hydrides mean for the dream of the discovery of high-temperature superconducting materials? Is there a limit to how high T_c can be in these conventional superconductors, and how does that limit depend on pressure, composition, and structure? Intuitively there should be a limit, after which superconductivity is out competed by structural distortion, compositional change, or other electronic or magnetic phases. Efforts in quantifying this will be valuable. Is extremely high pressure essential or might these results be opening our eyes to the possibility of room-temperature superconductivity under ambient, or close to ambient, conditions?

The wide range of T_c values predicted in superconducting hydrides (104), from few kelvins to above 300 K (see **Figure 10**), suggests that Ashcroft's remarkable idea (20, 36) was too general and that high T_c in hydrides is not just related to the Debye temperature being large. A strong electron–phonon coupling is also required. The range of λ in the hydrides is consequently also very large, with values from around 0.4 in PdH (74) to λ about 2 in H_3S (72, 76). A clear understanding of when a hydride yields a large λ will turn out to be crucial to clarify the prospects for the superconducting hydrides.

Superconductivity in the hydrides is forcing us to ponder what we mean by room temperature. One definition might be 0°C (273 K), but we can all agree that this would be a very cold room. Maybe 290 K is more reasonable, but we should remember that for technological applications the superconducting material would need to operate at well below T_c.

Of course, no room can be held at the megabar (100 GPa) pressures currently required to force the hydrides into the superconducting state. Indeed, as we have seen, these very high pressures mean that only very few experimental groups can participate in the search for new superconducting hydrides. It is essential that the pressures required are reduced. This could be promoted by computational predictions that seek a compromise and balance the pressure required with the T_c predicted, rather than simply trying to maximize T_c with no regard to the experimental conditions required. To this end, we propose a figure of merit, S, which makes the compromise explicit:

$$S = \frac{T_c}{\sqrt{T_{c,\mathrm{MgB_2}}^2 + P^2}}, \qquad 8.$$

where the temperatures are in Kelvin, and the pressures in gigapascal. This sets MgB_2 (a high-temperature conventional superconductor at ambient pressures, with technological applications) to have $S(MgB_2) = 1$. On this scale, a putative superconductor with a T_c of 390 K at ambient pressures (and so could be used without cooling or compression in a wide range of terrestrial conditions) would score a perfect $S(\star) = 10$. The current megabar superconducting hydrides have lower values (see **Figure 10**), reflecting the very high pressures required to achieve the superconducting phases—with both $S(H_3S)$ and $S(LaH_{10})$ equal to 1.3. A superconductor with a T_c of around 1,000 K at 100 GPa would score nearly 10 on this scale, which captures the astonishment that such a result would generate, and $S(HgBaCaCuO) = 3.5$ reflecting the Nobel Prize–worthy discovery of the cuprates.

An enduring puzzle is the disparity between the number of the theoretically predicted superconductors that now populate the literature and the few that have been experimentally realized. As mentioned above, this may partly be due to the relatively few groups that can currently perform the necessary experiments. But it is not the whole story, and it would be helpful if theoretical predictions could comment on the likely ease (or otherwise) of experimental synthesis. As the experimental evidence reviewed here suggests, large kinetic barriers appear to be hindering the synthesis of the superconducting hydrides.

As was seen with the early investigations of compressed silane and the decomposition of H_2O, more stable structures or compositions will typically have lower densities of electronic states at the Fermi level, reducing the prospects of high-temperature superconductivity. This leads to a potential bias in the predictions toward higher T_c. It is not possible to guarantee that a ground-state structure has been identified in any stochastic search, but searches halted too soon (for example, when a pleasing result has been obtained) are potentially unreliable.

On the computational side, the high-throughput sweep of databases or stochastic searches has become relatively routine. However, the computation of T_c has not. The most reliable results require care (110) and very large computational resources. This becomes even more the case if anharmonic effects, which we have seen are important for hydrogen-containing compounds, are to be computed. Progress in this direction, particularly the automation of the computations, would advance the field considerably.

Unconventional superconductivity may also be encountered in high-pressure experiments. Unfortunately, predictive computational methods are not currently helpful in this case. Should quantitative theories emerge for unconventional superconducting states, we could look forward to the same fruitful symbiosis between theory, computation, and experiment that has been so successful for the superconducting hydrides.

15. CONCLUSION

The existence of high temperatures superconductivity in metallic hydrogen, or hydrogen rich compounds, has long been theoretically discussed and in 2014 superconductivity was discovered in compressed hydrogen sulfide at 203 K and around 150 GPa. In 2018 superconductivity was observed in compressed lanthanum hydride at above 250 K and around 200 GPa by two independent groups. First-principles structure and superconductivity predictions have played a crucial role in guiding these experimental discoveries. A detailed theoretical picture of the superconducting mechanism has emerged for H_3S, and it is expected to do so for LaH_{10}.

Experiments involving hydrogen at megabar pressures are extremely challenging. In view of the recent discoveries, the theoretical effort will continue in the coming years with the hope of leading the design of more accessible high temperature superconducting hydrides. However, mindful of the apparently singular success of MgB_2, are we at risk of being misled that there are many more such superconductors to be discovered at ambient pressure? Can a similar combination of theory and computation lead to the discovery of new high-T_c superconductors beyond the hydrides at technologically relevant conditions?

DISCLOSURE STATEMENT

C.J.P. is an author of the CASTEP code and receives royalty payments from its commercial sales by Dassault Systèmes. The authors are otherwise not aware of any affiliations, memberships, funding, or financial holdings that might be perceived as affecting the objectivity of this review.

ACKNOWLEDGMENTS

C.J.P. is supported by the Royal Society through a Royal Society Wolfson Research Merit award. I.E. has received funding from the European Research Council (ERC) under the European Union's Horizon 2020 research and innovation program (grant agreement No. 802533), and the Spanish Ministry of Economy and Competitiveness (FIS2016-76617-P). M.I.E. thanks the Max Planck community for invaluable support, and U. Pöschl for the constant encouragement. We thank Joseph Nelson for a careful reading of the manuscript.

LITERATURE CITED

1. Van Delft D, Kes P. 2010. *Phys. Today* 63:38–43
2. Meissner W, Ochsenfeld R. 1933. *Naturwissenschaften* 21:787–88
3. Drozdov AP, Eremets MI, Troyan IA, Ksenofontov V, Shylin SI. 2015. *Nature* 525:73–76
4. Drozdov AP, Kong PP, Minkov VS, Besedin SP, Kuzovnikov MA, et al. 2019. *Nature* 569:528–31
5. Matthias B, Geballe T, Geller S, Corenzwit E. 1954. *Phys. Rev.* 95:1435
6. London F, London H. 1935. *Proc. R. Soc. Lond. Ser. A-Math. Phys. Sci.* 149:71–88
7. Maxwell E. 1950. *Phys. Rev.* 79:173
8. Reynolds C, Serin B, Wright W, Nesbitt L. 1950. *Phys. Rev.* 78:487
9. Bardeen J, Cooper LN, Schrieffer JR. 1957. *Phys. Rev.* 106:162
10. Bardeen J, Cooper LN, Schrieffer JR. 1957. *Phys. Rev.* 108:1175
11. Wigner E, Huntington HB. 1935. *J. Chem. Phys.* 3:764–70
12. McMahon JM, Morales MA, Pierleoni C, Ceperley DM. 2012. *Rev. Mod. Phys.* 84:1607
13. Zaghoo M, Silvera IF. 2017. *PNAS* 114:11873–77
14. Celliers PM, Millot M, Brygoo S, McWilliams RS, Fratanduono DE, et al. 2018. *Science* 361:677–82
15. Knudson MD, Desjarlais MP, Becker A, Lemke RW, Cochrane KR, et al. 2015. *Science* 348:1455–60
16. Dias RP, Silvera IF. 2017. *Science* 355:715–18
17. Cudazzo P, Profeta G, Sanna A, Floris A, Continenza A, et al. 2008. *Phys. Rev. Lett.* 100:257001
18. Monserrat B, Drummond ND, Dalladay-Simpson P, Howie RT, Ríos PL, et al. 2018. *Phys. Rev. Lett.* 120:255701
19. Azadi S, Monserrat B, Foulkes WMC, Needs RJ. 2014. *Phys. Rev. Lett.* 112:165501
20. Ashcroft NW. 1968. *Phys. Rev. Lett.* 21:1748
21. Pickard CJ, Needs RJ. 2007. *Nat. Phys.* 3:473
22. Merriam M, Schreiber D. 1963. *J. Phys. Chem. Solids* 24:1375–77
23. Gupta M, Burger J. 1980. *Phys. Rev. B* 22:6074
24. Satterthwaite CB, Toepke IL. 1970. *Phys. Rev. Lett.* 25:741–43
25. Skoskiewicz T. 1973. *Phys. Status Solidi (b)* 59:329–34
26. Stritzker B, Buckel W. 1972. *Z. Phys. A Hadrons Nuclei* 257:1–8
27. Bednorz JG, Müller KA. 1986. *Z. Phys. B Condens. Matter* 64:189–93
28. Gao L, Xue YY, Chen F, Xiong Q, Meng RL, et al. 1994. *Phys. Rev. B* 50:4260–63
29. Zaanen J. 2010. In *100 Years of Superconductivity*, ed. H Rogalla, PH Kes, pp. 92–114. Boca Raton, FL: CRC Press
30. Kamihara Y, Hiramatsu H, Hirano M, Kawamura R, Yanagi H, et al. 2006. *J. Am. Chem. Soc.* 128:10012–13
31. Kamihara Y, Watanabe T, Hirano M, Hosono H. 2008. *J. Am. Chem. Soc.* 130:3296–97
32. Vojta M. 2003. *Rep. Progress Phys.* 66:2069
33. Nagamatsu J, Nakagawa N, Muranaka T, Zenitani Y, Akimitsu J. 2001. *Nature* 410:63–64
34. Tomsic M, Rindfleisch M, Yue J, McFadden K, Phillips J, et al. 2007. *Int. J. Appl. Ceram. Technol.* 4:250–59
35. Weller TE, Ellerby M, Saxena SS, Smith RP, Skipper NT. 2005. *Nat. Phys.* 1:39–41
36. Ashcroft NW. 2004. *Phys. Rev. Lett.* 92:187002
37. Feng J, Grochala W, Jaroń T, Hoffmann R, Bergara A, Ashcroft NW. 2006. *Phys. Rev. Lett.* 96:017006
38. Capitani F, Langerome B, Brubach JB, Roy P, Drozdov A, et al. 2017. *Nat. Phys.* 13:859–63
39. Hohenberg P, Kohn W. 1964. *Phys. Rev.* 136:B864–71
40. Kohn W, Sham LJ. 1965. *Phys. Rev.* 140:A1133–38
41. Perdew JP, Burke K, Ernzerhof M. 1996. *Phys. Rev. Lett.* 77:3865–68
42. Needs RJ, Pickard CJ. 2016. *APL Mater.* 4:053210
43. Oganov AR, Glass CW. 2006. *J. Chem. Phys.* 124:244704
44. Pickard CJ, Needs RJ. 2006. *Phys. Rev. Lett.* 97:045504
45. Clark SJ, Segall MD, Pickard CJ, Hasnip PJ, Probert MI, et al. 2005. *Z. Krist. Cryst. Mater.* 220:567–70
46. Kresse G, Furthmüller J. 1996. *Phys. Rev. B* 54:11169
47. Pickard CJ, Needs RJ. 2011. *J. Phys.: Condens. Matter* 23:053201

48. Wang Y, Lv J, Zhu L, Ma Y. 2012. *Comput. Phys. Commun.* 183:2063–70
49. Li Y, Wang L, Liu H, Zhang Y, Hao J, et al. 2016. *Phys. Rev. B* 93:020103
50. Peng F, Sun Y, Pickard CJ, Needs RJ, Wu Q, Ma Y. 2017. *Phys. Rev. Lett.* 119:107001
51. Giannozzi P, Baroni S, Bonini N, Calandra M, Car R, et al. 2009. *J. Phys.: Condens. Matter* 21:395502
52. Lejaeghere K, Bihlmayer G, Björkman T, Blaha P, Blügel S, et al. 2016. *Science* 351:aad3000
53. Oganov A, Pickard CJ, Zhu Q, Needs RJ. 2019. *Nat. Rev. Mater.* 4:331–48
54. Jain A, Shin Y, Persson KA. 2016. *Nat. Rev. Mater.* 1:15004
55. Zhang L, Wang Y, Lv J, Ma Y. 2017. *Nat. Rev. Mater.* 2:17005
56. Eremets M, Troyan I. 2011. *Nat. Mater.* 10:927
57. Howie RT, Guillaume CL, Scheler T, Goncharov AF, Gregoryanz E. 2012. *Phys. Rev. Lett.* 108:125501
58. Feng J, Hennig RG, Ashcroft N, Hoffmann R. 2008. *Nature* 451:445
59. Pickard CJ, Martinez-Canales M, Needs RJ. 2013. *Phys. Rev. Lett.* 110:245701
60. Giustino F. 2017. *Rev. Mod. Phys.* 89:015003
61. Baroni S, de Gironcoli S, Dal Corso A, Giannozzi P. 2001. *Rev. Mod. Phys.* 73:515–62
62. Frederiksen T, Paulsson M, Brandbyge M, Jauho AP. 2007. *Phys. Rev. B* 75:205413
63. Mauri F, Zakharov O, de Gironcoli S, Louie SG, Cohen ML. 1996. *Phys. Rev. Lett.* 77:1151–54
64. Monserrat B. 2018. *J. Phys.: Condens. Matter* 30:083001
65. Allen PB, Dynes RC. 1975. *Phys. Rev. B* 12:905–22
66. Sanna A, Flores-Livas JA, Davydov A, Profeta G, Dewhurst K, et al. 2018. *J. Phys. Soc. Jpn.* 87:041012
67. Yildirim T, Gülseren O, Lynn JW, Brown CM, Udovic TJ, et al. 2001. *Phys. Rev. Lett.* 87:037001
68. Calandra M, Mauri F. 2005. *Phys. Rev. Lett.* 95:237002
69. Calandra M, Mauri F. 2008. *Phys. Rev. Lett.* 101:016401
70. Allen PB, Mitrovicć B. 1983. In *Solid State Physics*, Vol. 37, ed. H Ehrenreich, F Seitz, D Turnbull, pp. 1–92. New York: Academic
71. Oliveira LN, Gross EKU, Kohn W. 1988. *Phys. Rev. Lett.* 60:2430–33
72. Errea I, Calandra M, Pickard CJ, Nelson J, Needs RJ, et al. 2015. *Phys. Rev. Lett.* 114:157004
73. Rousseau B, Bergara A. 2010. *Phys. Rev. B* 82:104504
74. Errea I, Calandra M, Mauri F. 2013. *Phys. Rev. Lett.* 111:177002
75. Errea I, Calandra M, Mauri F. 2014. *Phys. Rev. B* 89:064302
76. Errea I, Calandra M, Pickard CJ, Nelson JR, Needs RJ, et al. 2016. *Nature* 532:81
77. Sano W, Koretsune T, Tadano T, Akashi R, Arita R. 2016. *Phys. Rev. B* 93:094525
78. Borinaga M, Riego P, Leonardo A, Calandra M, Mauri F, et al. 2016. *J. Phys.: Condens. Matter* 28:494001
79. Borinaga M, Errea I, Calandra M, Mauri F, Bergara A. 2016. *Phys. Rev. B* 93:174308
80. Scheler T, Degtyareva O, Marqués M, Guillaume CL, Proctor JE, et al. 2011. *Phys. Rev. B* 83:214106
81. Eremets M, Trojan I, Medvedev S, Tse J, Yao Y. 2008. *Science* 319:1506–9
82. Gao G, Oganov AR, Bergara A, Martinez-Canales M, Cui T, et al. 2008. *Phys. Rev. Lett.* 101:107002
83. Pickard CJ, Needs R. 2007. *Phys. Rev. B* 76:144114
84. Goncharenko I, Eremets M, Hanfland M, Tse J, Amboage M, et al. 2008. *Phys. Rev. Lett.* 100:045504
85. Wang H, John ST, Tanaka K, Iitaka T, Ma Y. 2012. *PNAS* 109:6463–66
86. Li Y, Hao J, Liu H, Li Y, Ma Y. 2014. *J. Chem. Phys.* 140:174712
87. Ma Y, Eremets M, Oganov AR, Xie Y, Trojan I, et al. 2009. *Nature* 458:182
88. Duan D, Liu Y, Tian F, Li D, Huang X, et al. 2014. *Sci. Rep.* 4:6968
89. Liu H, Naumov II, Hoffmann R, Ashcroft N, Hemley RJ. 2017. *PNAS* 114:6990–95
90. Duan D, Huang X, Tian F, Li D, Yu H, et al. 2015. *Phys. Rev. B* 91:180502
91. Akashi R, Kawamura M, Tsuneyuki S, Nomura Y, Arita R. 2015. *Phys. Rev. B* 91:224513
92. Flores-Livas JA, Sanna A, Gross EK. 2016. *Eur. Phys. J. B* 89:63
93. Akashi R, Sano W, Arita R, Tsuneyuki S. 2016. *Phys. Rev. Lett.* 117:075503
94. Bianco R, Errea I, Calandra M, Mauri F. 2018. *Phys. Rev. B* 97:214101
95. Einaga M, Sakata M, Ishikawa T, Shimizu K, Eremets MI, et al. 2016. *Nat. Phys.* 12:835–38
96. Goncharov AF, Lobanov SS, Prakapenka VB, Greenberg E. 2017. *Phys. Rev. B* 95:140101
97. Guigue B, Marizy A, Loubeyre P. 2017. *Phys. Rev. B* 95:020104
98. Troyan I, Gavriliuk A, Rüffer R, Chumakov A, Mironovich A, et al. 2016. *Science* 351:1303–6

99. Mozaffari S, Sun D, Minkov VS, Drozdov AP, Knyazev D, et al. 2019. *Nat. Commun.* 10:2522
100. Schirber JE, Northrup CJM. 1974. *Phys. Rev. B* 10:3818–20
101. Somayazulu M, Ahart M, Mishra AK, Geballe ZM, Baldini M, et al. 2019. *Phys. Rev. Lett.* 122:027001
102. Schilling A, Cantoni M, Guo JD, Ott HR. 1993. *Nature* 363:56–58
103. Wu G, Xie YL, Chen H, Zhong M, Liu RH, et al. 2009. *J. Phys.: Condens. Matter* 21:142203
104. Bi T, Zarifi N, Terpstra T, Zurek E. 2019. In *Reference Module in Chemistry, Molecular Sciences and Chemical Engineering*. **https://doi.org/10.1016/B978-0-12-409547-2.11435-0**
105. Drozdov AP, Eremets MI, Troyan IA. 2015. *arXiv e-prints*: arXiv:1508.06224
106. Flores-Livas JA, Amsler M, Heil C, Sanna A, Boeri L, et al. 2016. *Phys. Rev. B* 93:020508
107. Drozdov AP, Minkov VS, Besedin SP, Kong PP, Kuzovnikov MA, et al. 2018. *arXiv e-prints*: arXiv:1808.07039
108. Geballe ZM, Liu H, Mishra AK, Ahart M, Somayazulu M, et al. 2018. *Angew. Chem. Int. Ed.* 57:688–92
109. Hirsch JE. 2009. *Phys. Scr.* 80:035702
110. Zarifi N, Bi T, Liu H, Zurek E. 2018. *J. Phys. Chem. C* 122:24262–69